Developmental Cell, Vol. 7, 763–769, November, 2004, Copyright ©2004 by Cell Press

RGS14 Is a Mitotic Spindle Protein Essential from the First Division of the Mammalian Zygote

Short Article

Luke Martin-McCaffrey,[1] Francis S. Willard,[2] Antonio J. Oliveira-dos-Santos,[3] David R.C. Natale,[1,6] Bryan E. Snow,[4] Randall J. Kimple,[2] Agnieszka Pajak,[1] Andrew J. Watson,[1] Lina Dagnino,[1] Josef M. Penninger,[5,*] David P. Siderovski,[2,*] and Sudhir J.A. D'Souza[1,*]

[1]Department of Physiology and Pharmacology
Schulich School of Medicine
University of Western Ontario
London, Ontario N6A 5C1
Canada

[2]Department of Pharmacology
UNC Lineberger Comprehensive Cancer Center
University of North Carolina
Chapel Hill, North Carolina 27599

[3]AMGEN
Cambridge Research Center
Cambridge, Massachusetts 02139

[4]Ontario Cancer Institute
University of Toronto
Toronto, Ontario M5G 2M9
Canada

[5]IMBA
Institute for Molecular Biotechnology of the Austrian Academy of Sciences
Dr. Bohr-Gasse 3-5
1030 Vienna
Austria

Summary

Heterotrimeric G protein α subunits, RGS proteins, and GoLoco motif proteins have been recently implicated in the control of mitotic spindle dynamics in *C. elegans* and *D. melanogaster*. Here we show that "regulator of G protein signaling-14" (RGS14) is expressed by the mouse embryonic genome immediately prior to the first mitosis, where it colocalizes with the anastral mitotic apparatus of the mouse zygote. Loss of *Rgs14* expression in the mouse zygote results in cytofragmentation and failure to progress to the 2-cell stage. RGS14 is found in all tissues and segregates to the nucleus in interphase and to the mitotic spindle and centrioles during mitosis. Alteration of RGS14 levels in exponentially proliferating cells leads to cell growth arrest. Our results indicate that RGS14 is one of the earliest essential product of the mammalian embryonic genome yet described and has a general role in mitosis.

*Correspondence: josef.penninger@imba.oeaw.ac.at (J.M.P.), dsiderov@med.unc.edu (D.P.S.), sjdsouza@uwo.ca (S.J.A.D.)

[6]Present address: Department of Biochemistry and Molecular Biology, Genes and Development Research Group, University of Calgary, Health Sciences Centre, Calgary AB T2N 4N1, Canada.

Introduction

Heterotrimeric guanine-nucleotide binding proteins (G proteins) transduce extracellular signals received from heptahelical (7TM) cell surface receptors: upon activation of the heterotrimer by receptor-catalyzed guanine nucleotide exchange, the Gα·GTP and Gβγ subunits dissociate to propagate the signal intracellularly (Gilman, 1987). "Regulator of G protein signaling" (RGS) proteins accelerate the intrinsic guanosine triphosphatase (GTPase) activity of Gα and reformation of the heterotrimer; this "GTPase-accelerating protein" (GAP) activity of RGS proteins facilitates termination of receptor-evoked signaling (Neubig and Siderovski, 2002). Another class of Gα regulators, the GoLoco-motif proteins, act as guanine nucleotide dissociation inhibitors (GDIs) of GDP bound $G\alpha_i$ subunits, slowing their spontaneous GDP release and inhibiting reassociation of the heterotrimer (Willard et al., 2004).

Recent studies in *C. elegans* have uncovered roles for Gα and GoLoco proteins in the control of mitotic spindle force generation required for asymmetric cell division and embryogenesis (Gönczy, 2002). Asymmetry in the first cell division of the *C. elegans* zygote is achieved by a net imbalance of pulling forces acting on astral microtubules (MTs) (Gönczy, 2002). RNA interference (RNAi)-mediated knockdown of two *C. elegans* Gα orthologs (GOA-1 and GPA-16) or two GoLoco proteins (GPR-1 and GPR-2) leads to reduced and balanced pulling forces on the mitotic spindle, a resultant symmetric first division and, ultimately, embryonic death (Colombo et al., 2003; Gotta et al., 2003; Srinivasan et al., 2003). Disrupting the *C. elegans* gene *ric-8*, which encodes a nonreceptor guanine nucleotide exchange factor (GEF) for Gα subunits, also results in spindle misalignments and embryonic lethality (Afshar et al., 2004; Miller and Rand, 2000). Genetic studies in *D. melanogaster* have also implicated $G\alpha_i$ and the multi-GoLoco protein Partner of Inscuteable (Pins) in establishing cell polarity and asymmetric division (Cai et al., 2003; Schaefer et al., 2001). Similarly, LGN, the human ortholog of Pins, regulates spindle organization during mitosis (Du et al., 2001); disruption of spindle-pole organization and chromosome segregation occurs upon either overexpression or silencing of LGN expression (Du et al., 2002). Collectively, these findings suggest an evolutionary conservation of G protein α subunit involvement in MT dynamics critical for mitosis.

The mammalian protein RGS14 harbors a C-terminal GoLoco motif, which exerts GDI activity on GDP bound $G\alpha_i$ subunits (Kimple et al., 2002), as well as a RGS-box with $G\alpha_{i/o}$-directed GAP activity (Snow et al., 1997). Although several studies have examined the biochemical activity and regulation of RGS14 (e.g., Cho et al., 2000; Traver et al., 2000), none have determined its physiological function. Using a combination of gene-inactivation, constitutive expression, and RNAi knockdown strategies, we demonstrate that RGS14 is one of the earliest proteins elaborated by the mammalian genome,

A

Genotype:	+/+	+/-	-/-	p
Term	94	153	0	<0.001
E14.5	10	39	0	<0.001
E11.5	6	12	0	<0.001
E8.5	21	57	0	<0.001
E6.5	7	26	0	<0.001
Blast	30	68	0	<0.001
2-cell	34	59	4	<0.001
1-cell	10	12	5	n.s.

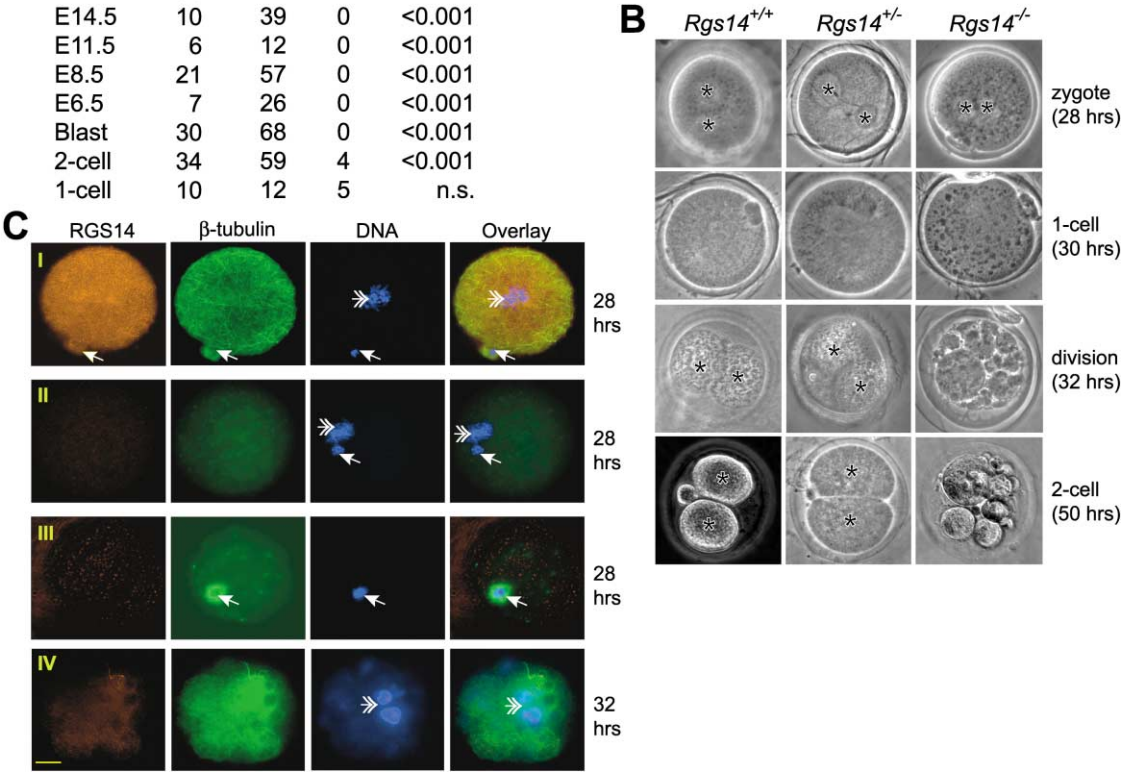

Figure 1. Targeted Inactivation of Mouse *Rgs14* Leads to Early Embryonic Lethality

(A) Observed genotypes of progeny of $Rgs14^{+/-} \times Rgs14^{+/-}$ matings in C57BL/6 and CD-1 backgrounds (all preimplantation progeny [1-cell, 2-cell, blastocysts] were from CD-1 background). p values indicate significant differences from expected Mendelian ratios; n.s., not significantly different from Mendelian ratio ($p = 0.335$).

(B) Bright field images of embryos collected 28 hr (zygote), 30 hr (1-cell), 32 hr (division), and 50 hr (2-cell) following hCG injection and mating. After microscopy, embryos were genotyped by nested PCR. Scale bar equals 10 μm. Asterisks denote pronuclei in 1-cell embryos and zygote nuclei in 2-cell embryos.

(C) Immunofluorescence analysis of 1-cell embryos of $Rgs14^{+/-}$ matings. Embryos from 28 and 32 hr after mating were immunostained for RGS14 (orange), β-tubulin (green), counterstained for DNA (blue), visualized by fluorescence microscopy, then genotyped by nested PCR. (I) A typical RGS14-positive embryo, exhibiting a well-defined MT network accompanied by condensed chromatin (double arrowhead) at the embryo center along the same plane as the polar body (solid white arrow). (II) An RGS14-negative embryo (28 hr) that lacks detectable MTs and has off-centered condensed chromatin (double arrowhead). (III) A RGS14-negative embryo (28 hr) that lacks an MT network but has small asters of MTs throughout. The polar body (solid white arrow) is detected, but embryonic DNA is a barely detectable bluish haze. (IV) An RGS14-negative embryo (32 hr) with a fragmented nucleus, diffuse DNA staining, and an ill-defined MT network. Scale bar equals 10 μm.

is critical for the first cell division of the fertilized zygote, and plays an essential role in mitosis.

Results and Discussion

$Rgs14^{-/-}$ Mice Fail to Progress Successfully through the First Zygotic Division

We constructed a deletional targeting vector for mouse *Rgs14* that eliminates exons 2 to 9, including those that encode the RGS-box (Supplemental Figure S1 at http://www.developmentalcell.com/cgi/content/full/7/5/763/DC1/). $Rgs14^{+/-}$ male and female mice were anatomically normal and fertile and indistinguishable from wild-type mice of the same strain. Matings of heterozygotes on C57BL/6 and CD-1 backgrounds produced 247 pups; 67.5% were $Rgs14^{+/-}$, but none were homozygous nulls (Figure 1A), demonstrating that the disruption of *Rgs14* leads to embryonic lethality. $Rgs14^{-/-}$ embryos were not detected among the progeny of $Rgs14^{+/-}$ matings isolated from time pregnancies between E6.5 and E14.5 and genotyped by nested PCR (Supplemental Figure S1). Dissection of embryos from implantation sites at E8.5 as well as histologic sections of uteri at E6.5 revealed no evidence of $Rgs14^{-/-}$ embryo resorption or empty decidua (data not shown), suggesting that *Rgs14* nulls fail either to implant or to reach the blastocyst stage.

We examined preimplantation progeny of timed $Rgs14^{+/-}$ matings by light and fluorescence microscopy prior to genotyping. $Rgs14^{-/-}$ embryos were first detected among the 97 2-cell embryos; however, at 4%, the frequency of the $Rgs14^{-/-}$ genotype was significantly less than the predicted Mendelian ratio (25%). Of the 27 1-cell embryos genotyped, 19% were $Rgs14^{-/-}$, 44% were $Rgs14^{+/-}$, and 37% were $Rgs14^{+/+}$, suggesting that

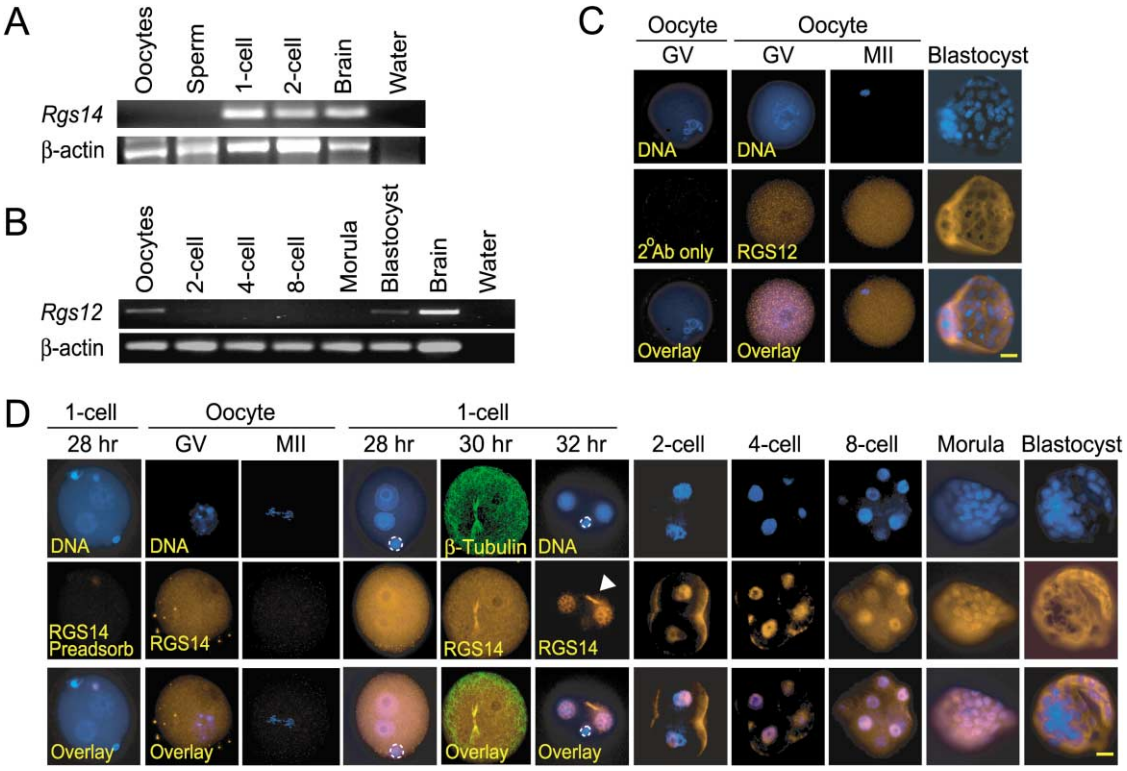

Figure 2. RGS14 Is Expressed De Novo after Fertilization as the Sole R12 Subfamily Member Expressed in Preimplantation Stages

(A and B) RT-PCR analyses of *Rgs14* (A) and *Rgs12* (B) expression in indicated gametes, preimplantation embryo stages, and adult mouse brain (as positive control). 1-cell and 2-cell embryos were isolated at 28 and 52 hr, respectively. cDNA integrity was confirmed using mouse β-*actin* primers (lower panels).

(C and D) Subcellular localization of RGS12 (C) and RGS14 (D) in oocytes (germinal vesicle [GV] or metaphase-II [MII] stages) and preimplantation embryo stages as examined by indirect immunofluorescence microscopy using rabbit anti-RGS12 or anti-RGS14-60 antiserum and Cy3-conjugated goat anti-rabbit secondary antibody (orange). DNA was counterstained with Hoechst 33258 dye (blue), except for the 1-cell zygote at 30 hr (D, middle), which was instead immunostained for β-tubulin (green) to reveal the anastral mitotic apparatus. Dotted circle: polar body. Arrowhead: microtubule-rich midbody. Scale bar equals 10 μm.

Rgs14 deficiency had impaired development by this stage in the homozygous null. 1- and 2-cell *Rgs14*$^{+/-}$ and *Rgs14*$^{+/+}$ embryos were healthy and indistinguishable by morphology (Figure 1B). In contrast, a significant fraction of nuclei in 1-cell *Rgs14*$^{-/-}$ embryos were blebbed and disorganized (Figure 1B), indicative of cytofragmentation. The non-Mendelian distribution of 1-cell embryos reflected difficulty in genotyping *Rgs14*$^{-/-}$ embryos by PCR given extensive DNA fragmentation and the general difficulty of genotyping single cells. It does not indicate a loss of heterozygotes because the predicted Mendelian ratio was consistently maintained during later stages.

Because of difficulty in genotyping *Rgs14*$^{-/-}$ embryos due to DNA fragmentation, we employed immunofluorescence microscopy to classify embryos as RGS14 positive or negative. We produced two rabbit antibodies directed against rat RGS14 fragments; antibody specificity was verified by immunoblot and immunocytochemistry on postimplantation mouse embryos and mouse trophoblast stem cells (Supplemental Figure S2). All RGS14-negative embryos successfully genotyped by nested RT-PCR (n = 30) were found to be *Rgs14*$^{-/-}$ and comprised 25% of the 1-cell progeny of *Rgs14*$^{+/-}$ crosses. The RGS14-positive embryos were found at different stages of mitosis, including late cytokinesis, and exhibited an organized MT network discernable by β-tubulin immunofluorescence (e.g., Figure 1C, I). In contrast, 46% of the RGS14-negative 1-cell embryos (19 of 41) exhibited condensed chromatin, which was misaligned or asymmetrically oriented with respect to the polar body (e.g., Figure 1C, II). Significantly, all 19 of the embryos with misaligned chromatin lacked detectable MTs (e.g., Figure 1C, II). The remainder (54%) exhibited very diffuse DNA staining and multiple foci of MTs arrayed throughout the cytoplasm (e.g., Figure 1C, III). The second polar body was found in all RGS14-negative embryos examined, demonstrating that meiosis is completed. However, neither the dense MTs about each pronuclei nor the barrel-shaped, anastral spindle was ever detected in *Rgs14*$^{-/-}$ embryos. By 32 hr postfertilization, 72% of RGS14-negative 1-cell embryos (37 of 52) were found to contain disorganized nuclei and hazy β-tubulin immunofluorescence (e.g., Figure 1C, IV).

Failure of *Rgs14*$^{-/-}$ embryos to survive past the first cell cycle following fertilization is surprising. Targeted inactivation of other genes expressed early in the zygote, such as *Hsp70* (Huang et al., 2001) and *MLL* (Ayton et al., 2001), either does not result in embryonic lethality or leads to embryonic death later in the preimplantation

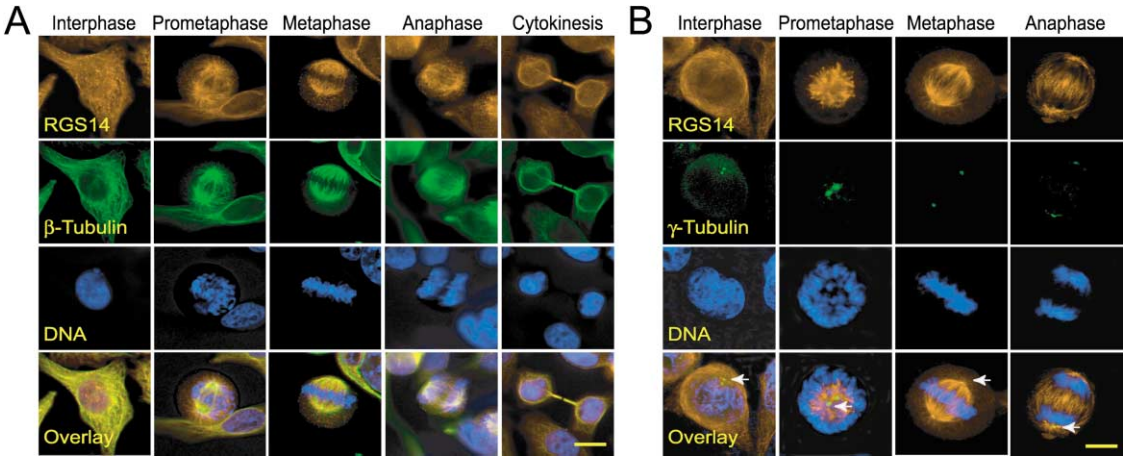

Figure 3. RGS14 Is Associated with the Mitotic Spindle, Midbody, and Centrioles in HeLa Cells

Distribution of RGS14 (orange), β-tubulin (green in [A]), or γ-tubulin (green in [B]) and DNA (blue) in synchronized HeLa cells fixed and stained with RGS14-60 and anti-β- or γ-tubulin antibodies and Hoechst 33258 dye, respectively, between 7 and 9 hr after release from a double-thymidine block. Colocalization of RGS14 and β- or γ-tubulin immunofluorescence is yellow in overlay. Scale bar equals 10 μm. Centrioles indicated by arrows.

period. We conclude that RGS14 is a critical regulator of mitotic progression by the mouse zygote.

Expression Analysis of *Rgs14* Transcript and Encoded Protein

The oocyte contains most of the proteins or the mRNA for the proteins required for the first and subsequent early divisions of the embryo (Schultz, 2002). To better understand why the loss of RGS14 results in so early an embryonic death, we examined RGS14 expression in gametes and early embryo stages (Figure 2). *Rgs14* mRNA was not detectable by RT-PCR in either sperm or oocyte but was readily amplified in the zygote through to the blastocyst stage (Figure 2A and data not shown). Maternal proteins may be present in the 1-cell embryo in the absence of the corresponding mRNA (Schultz, 2002). Consequently, we analyzed RGS14 protein expression in the preimplantation embryo. RGS14 is readily detected in germinal vesicle oocytes, but not in metaphase II oocytes (Figure 2D), suggesting that RGS14 is degraded during the second meiotic arrest of the oocytes.

Gamete cell cycles during meiosis involve successive M phases without an intervening S phase. Oocytes in most mammals undergo meiotic prophase entry in the fetal ovary, with all oocytes arresting in prophase by the time of birth. Competency to reinitiate and complete meiotic M phase is acquired to support the successive events of germinal vesicle breakdown, first polar body formation, arrest of meiosis at metaphase II, and completion of meiosis II upon fertilization. Whereas there appears to be sufficient RGS14 for completing the first meiotic division, none can be detected in the second meiotic arrest in metaphase II (Figure 2D), suggesting tight cell cycle-dependent regulation of RGS14 expression and a division in the factors required for each metaphase of the oocyte. Clearly, this raises the question as to how metaphase II is completed upon fertilization in the apparent absence of RGS14. Whether the other R12 subfamily member, RGS12, or another RGS protein may substitute for RGS14 to complete the second metaphase is unclear. Compellingly, *Rgs12* mRNA is detected in oocytes (Figure 2B) and RGS12 protein is detected by immunofluorescence in germinal vesicle and metaphase II oocytes (Figure 2C). RGS14 is elaborated in the zygote prior to the paternal and maternal chromosomes aligning in metaphase; the protein appears to associate with the perinuclear sheaths of MTs surrounding the pronuclei, prior to segregating to the anastral mitotic apparatus and subsequently the barrel-shaped cytoplasmic bridge between the nascent nuclei of the emerging 2-cell embryo (Figure 2D). RGS14 expression is detected continuously through the subsequent stages of the preimplantation embryo (Figure 2D). In contrast, RGS12 is below the level of detection in the zygote until the blastocyst stage (Figures 2B and 2C and data not shown). We conclude that *Rgs14* is transcribed and translated de novo by the embryonic genome prior to or at the time of initiation of the first cell cycle and persists throughout the preimplantation period, whereas its R12 subfamily relative *Rgs12* is not transcribed until later stages of embryogenesis. Consequently, there is no compensation for the targeted inactivation of *Rgs14* in the zygote.

RGS14 Is an Ubiquitious and Essential Regulator of MTs and the Mitotic Spindle

Others have reported that RGS14 expression is limited to the spleen and the brain (Cho et al., 2000; Traver et al., 2000). In contrast, we have detected RGS14 expression throughout mouse embryogenesis and in all mouse tissues from E7.5 through to adulthood (e.g., Figure 2D, Supplemental Figure S2). Our finding of RGS14 protein expression in a variety of adult mouse tissues (Supplemental Figure S2) is consistent with our previously reported Northern blot analysis in the rat which demonstrated that, whereas *RGS14* mRNA was abundant in spleen and brain, lower expression was readily detectable in all other adult rat tissues examined (Snow et al.,

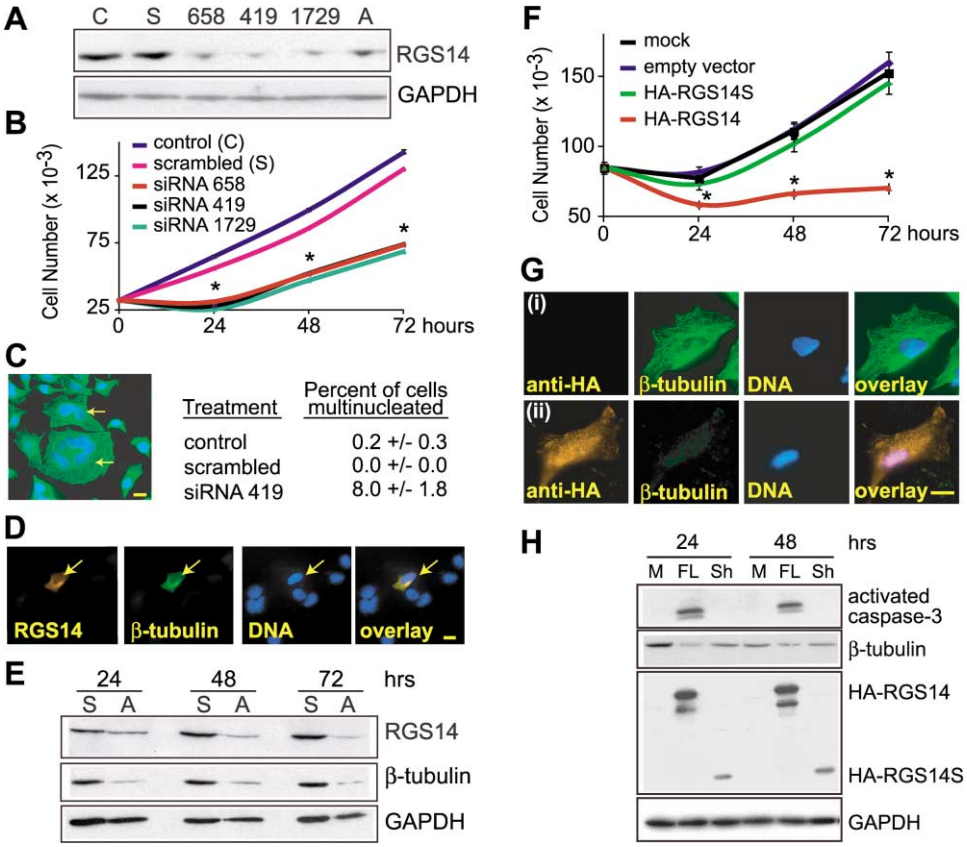

Figure 4. Alterations in RGS14 Expession Levels Are Deleterious to HeLa Cells

(A) Knockdown of RGS14 protein levels in cells transfected with three different *hRGS14*-directed siRNAs (419, 658, 1729) either individually or in a single pool (A). Lipofection reagent alone (C) nor a scrambled siRNA (S) affected RGS14 levels. The immunoblot was reprobed for GAPDH to confirm equal loading.

(B) RGS14 knockdown decreases cell proliferation. HeLa cultures were counted over 72 hr following transfection with indicated *hRGS14* siRNA or controls (*$p < 0.01$, analysis of variance, $n = 8$).

(C) RGS14 knockdown induces multinucleated cells. Cells were fixed 48 hr posttransfection with siRNA 419, stained with anti-β-tubulin (green) and Hoechst 33258 dye (blue). siRNA 419 transfection gave a significant increase in cells with two or more nuclei (arrows). Scale bar equals 50 μm.

(D) Abolition of RGS14 expression eliminates β-tubulin immunofluorescence. Cells were fixed 24 hr posttransfection with siRNA 1729 and stained for RGS14 (orange), β-tubulin (green), and DNA content (blue). In cells with RGS14 immunofluorescence reduced below the detection limit, MTs were also not detected. Cells retaining demonstrable RGS14 expression (arrow) also exhibited β-tubulin immunoreactivity. Scale bar equals 10 μm.

(E) RGS14 knockdown produces concomitant decrease in β-tubulin levels. Cell cultures were transfected with three *hRGS14*-directed siRNAs in a single pool (A). Note that the scrambled siRNA (S) did not affect the abundance of either RGS14 or β-tubulin as detected by immunoblotting of cell lysates.

(F) Cell number over 72 hr in cultures transiently transfected with pcDNA3.1 vectors expressing HA-epitope tagged full-length (HA-RGS14) and short splice variant RGS14 (HA-RGS14S) or empty vector or liposomes only (mock). (*$p < 0.01$, analysis of variance, $n = 4$).

(G) Cell cultures, transiently transfected with either (i) empty vector or (ii) pcDNA3.1-HA-RGS14 were fixed and probed with anti-HA (orange) and anti-β-tubulin (green) antibodies and counterstained for DNA (blue). Cells positive for HA-RGS14 protein expression (e.g., bottom left) do not exhibit β-tubulin immunofluorescence.

(H) Activated caspase-3 and β-tubulin content in whole-cell lysates after transient transfection with either empty vector (M), pcDNA3.1-HA-RGS14 (FL), or pcDNA3.1-HA-RGS14S (Sh) and immunoblotted at indicated times posttransfection.

1997). This expression pattern suggests that RGS14 may be involved in critical cell division processes irrespective of cell type. We thus examined RGS14 expression in several exponentially proliferating cell lines, including HeLa cells, COS-7 cells, dermal fibroblasts, and trophoblast stem cells. Although a clear cytoplasmic signal associated with the microtubule-organizing center and MTs is often present, RGS14 is found in the nucleus during interphase and segregates to the centrosomes and astral MTs during mitosis (e.g., Figure 3 and Supplemental Figure S3 for HeLa cells). Thus, we conclude that RGS14 is ubiquitously expressed and likely plays a general role in the organization of MTs in interphase and in mitosis.

To further elucidate the actions of RGS14, we decreased endogenous RGS14 levels in cultured HeLa cells using siRNA. Three siRNAs were transfected either individually or in a single pool into exponentially proliferating, synchronized HeLa cells. Each of the siRNAs, either independently or pooled, but neither transfection reagent alone nor a scrambled siRNA reduced considerably the abundance of RGS14 protein within 24 hr of

transfection (Figure 4A). siRNA-induced knockdown of RGS14 levels decreased cell proliferation (Figure 4B) and induced an 80-fold increase in multinucleated cells (Figure 4C). Multiple micronuclei in a single cell reflects abnormal chromosomal segregation and was observed in response to both siRNA-induced knockdown and constitutive expression of the GoLoco motif-containing protein LGN (Du et al., 2001). Low levels of RGS14 protein were detectable by immunofluorescence in 90% of cells transfected with siRNAs. When, on occasion, siRNA treatment decreased RGS14 abundance below our detection limit, MTs were not visible by immunofluorescence (Figure 4D), similar to our findings with *Rgs14*$^{-/-}$ embryos. Similarly, the abundance of β-tubulin decreased in siRNA-treated cell cultures for up to 72 hr posttransfection (Figure 4E).

We also determined the effect of increased RGS14 expression. Two splice variants of RGS14 have been described, including one termed RGS14-short or "RGS14S" (GenBank AF037194), in which the RGS-box and GoLoco motif are truncated and deleted, respectively. Constitutive expression of full-length RGS14, but not RGS14S, caused cell death (Figure 4F). Exogenous expression of full-length RGS14 also resulted in a loss of the cellular MT network (Figure 4G) and decreased the abundance of β-tubulin (Figure 4H) but did not produce a significant increase in the number of multinucleated cells. These data suggest that the relative abundance of full-length RGS14 is crucial to its function, with either constitutive expression or siRNA-mediated elimination abrogating normal MT dynamics; these findings parallel those with LGN overexpression and siRNA knockdown (Du et al., 2001).

Significantly, constitutive expression of RGS14S does not affect cell proliferation or MTs (Figures 4F–4H), suggesting that the action of RGS14 in microtubule dynamics may be to modulate the nucleotide cycling of Gα subunits with its RGS-box and GoLoco motif. This is consistent with the phenotypes induced by inactivation of Gα subunits or their associated nucleotide-state modulators in *C. elegans* and *D. melanogaster*—findings that suggest the existence of a Gα nucleotide cycle distinct from that traditionally associated with 7TM receptors (Willard et al., 2004). We and others have identified two Gα subunits (GOA-1, GPA-16), two GoLoco proteins (GPR-1, GPR-2), an RGS protein (RGS-7), and a receptor-independent GEF (RIC-8) as critical components in generating astral MT force required for asymmetric cell division of *C. elegans* zygotes (Afshar et al., 2004; Colombo et al., 2003; Gotta et al., 2003; Hess et al., 2004; Srinivasan et al., 2003). Although there is yet no evidence that mammalian Ric-8A (Tall et al., 2003) is associated with the mitotic apparatus in mammalian cells, either it or an equivalent GEF may act in concert with RGS14. Future studies should define the various interactions between RGS14, $G\alpha_i$, tubulin, Ric-8, and/or other Gα regulators in mitotic spindle organization and chromosomal segregation in mammalian cells.

Experimental Procedures

Reagents

Unless specified, all reagents were purchased from Sigma. HA-tagged rat RGS14 (Snow et al., 1997) was subcloned into pcDNA3.1 (Invitrogen, San Diego, CA). HA-tagged RGS14S was purchased from the UMR cDNA Resource Center. Mouse anti-β-tubulin monoclonal antibody (E7) was obtained from the Developmental Studies Hybridoma Bank (The University of Iowa, Iowa City, IA). Other antibodies used were HA (12CA5 Roche, Indianapolis, IN), activated caspase-3 (Cell Signaling, Beverly, MA), γ-tubulin (Sigma), and GAPDH (Biogenesis, Kingston, NH).

Embryo and Oocyte Immunofluorescence

Preimplantation and postimplantation embryos were isolated as described (Hogan et al., 1994). Germinal vesicle stage and metaphase II oocytes were isolated from 16-week superovulated mice as described (Lee et al., 2004).

Flushed embryos were immobilized, fixed, and permeabilized as previously described (Hunt et al., 1995). Embryos were incubated for 1 hr with primary antibodies (anti-RGS14-60, 1:250; β-tubulin, 1:10; γ-tubulin, 1:250 dilution in 5% goat serum), washed, and incubated with Cy3-, FITC-, or Alexa 488-conjugated goat anti-rabbit or anti-mouse antibodies (Molecular Probes, Portland, OR) for 1 hr. Before mounting in anti-fade Permamount (DAKO, Denmark), embryos were washed and incubated for 15 min with Hoescht 33258 (10 μg/ml) (Sigma). All washes were performed at room temperature or 37°C using PBST (PBS + 0.1% Triton X-100) with frequent changes over 60 min. To visualize MTs, embryos were fixed in MT stabilization and fixation buffer (20 mM PIPES [pH 7.0], 1 mM $MgCl_2$, 0.5 mM EGTA, 1 mM DTT, 1 μg/ml aprotinin, 2 mM taxol, 0.1% Triton X-100, 2% formaldehyde) at 37°C for 30 min and probed with mouse anti-β−tubulin antibodies.

Microscopy

Fluorescence and brightfield images were collected digitally on a fully automated inverted microscope (DMIRB, Leica, Germany) connected to a Orca II digital camera (Hammamatsu, Japan) controlled by Openlab 2.2 Digital Image Analysis software (Improvision, Coventry, UK) run on a Mac G4 (Apostolova et al., 2002). Serial Z-plane sections were deconvolved using the same system.

Cell Culture

HeLa cells (ATCC, Manassas, VA) grown in Dulbecco's modified essential medium (DMEM) (Invitrogen) supplemented with 8% fetal bovine serum (FBS) were synchronized with a double-thymidine block (2 mM thymidine, 16 hr) as previously described (Schweitzer and D'Souza-Schorey, 2002). To examine cells at different stages of mitosis, HeLa cells released between 7 and 10 hr from the second thymidine block were isolated at 15–30 min intervals and fixed at 4°C in 2% paraformaldehyde (PFA)/0.1% Triton X-100 in PBS.

RNA Interference and cDNA Transfection

Three siRNAs corresponding to base pairs 419–441, 658–679, and 1729–1750 of human *RGS14* cDNA (GenBank NM_006480) were made with the Silencer siRNA construction kit as per manufacturer's directions (Ambion, Austin, TX). A scrambled siRNA based on a random sequence with no known homology was also generated. Lipofectamine 2000 (Invitrogen) was used to transfect either individual or pooled siRNAs and HA-RGS14 and HA-RGS14S pcDNA3.1 plasmids into HeLa cells following the manufacturer's instructions. HeLa cells were isolated and lysed and the ensuing protein lysates resolved by SDS-PAGE and immunoblotting as described (Apostolova et al., 2002).

Acknowledgments

We thank Dr. P. Hunt, B. Wolfe, and M. Welsh for assistance and Drs. G.M. Kidder and C. McCudden for critical appraisal of the manuscript. The Heart and Stroke Foundation of Ontario (T5051 to S.J.A.D.) and NIH GM062338 (to D.P.S.) provided support for the work. L.M.-M. and D.R.C.N. both acknowledge OGS studentships. F.S.W. is a postdoctoral fellow of the American Heart Association. R.J.K. acknowledges predoctoral fellowship support from the NIMH F30 MH64319. S.J.A.D. is a Canadian Institutes of Health Research New Investigator. J.M.P. is supported by IMBA, the Austrian Academy of Sciences, and a grant from the Austrian National Bank.

Received: April 30, 2004
Revised: September 20, 2004
Accepted: October 5, 2004
Published: November 8, 2004

References

Afshar, K., Willard, F.S., Colombo, K., Johnston, C.A., McCudden, C.R., Siderovski, D.P., and Gönczy, P. (2004). RIC-8 is required for GPR-1/2-dependent G-alpha function during asymmetric division of *C. elegans* embryos. Cell *119*, 219–230.

Apostolova, M.D., Ivanova, I.A., Dagnino, C., D'Souza, S.J., and Dagnino, L. (2002). Active nuclear import and export pathways regulate E2F-5 subcellular localization. J. Biol. Chem. *277*, 34471–34479.

Ayton, P., Sneddon, S.F., Palmer, D.B., Rosewell, I.R., Owen, M.J., Young, B., Presley, R., and Subramanian, V. (2001). Truncation of the Mll gene in exon 5 by gene targeting leads to early preimplantation lethality of homozygous embryos. Genesis *30*, 201–212.

Cai, Y., Yu, F., Lin, S., Chia, W., and Yang, X. (2003). Apical complex genes control mitotic spindle geometry and relative size of daughter cells in *Drosophila* neuroblast and pI asymmetric divisions. Cell *112*, 51–62.

Cho, H., Kozasa, T., Takekoshi, K., De Gunzburg, J., and Kehrl, J.H. (2000). RGS14, a GTPase-activating protein for Gialpha, attenuates Gialpha- and G13alpha-mediated signaling pathways. Mol. Pharmacol. *58*, 569–576.

Colombo, K., Grill, S.W., Kimple, R.J., Willard, F.S., Siderovski, D.P., and Gonczy, P. (2003). Translation of polarity cues into asymmetric spindle positioning in *Caenorhabditis elegans* embryos. Science *300*, 1957–1961.

Du, Q., Stukenberg, P.T., and Macara, I.G. (2001). A mammalian Partner of inscuteable binds NuMA and regulates mitotic spindle organization. Nat. Cell Biol. *3*, 1069–1075.

Du, Q., Taylor, L., Compton, D.A., and Macara, I.G. (2002). LGN blocks the ability of NuMA to bind and stabilize microtubules. A mechanism for mitotic spindle assembly regulation. Curr. Biol. *12*, 1928–1933.

Gilman, A.G. (1987). G proteins: transducers of receptor-generated signals. Annu. Rev. Biochem. *56*, 615–649.

Gönczy, P. (2002). Mechanisms of spindle positioning: focus on flies and worms. Trends Cell Biol. *12*, 332–339.

Gotta, M., Dong, Y., Peterson, Y.K., Lanier, S.M., and Ahringer, J. (2003). Asymmetrically distributed *C. elegans* homologs of AGS3/PINS control spindle position in the early embryo. Curr. Biol. *13*, 1029–1037.

Hess, H.A., Röper, J.-C., Grill, S.W., and Koelle, M.R. (2004). RGS-7 completes a receptor-independent heterotrimeric G protein cycle to asymmetrically regulate mitotic spindle positioning in *C. elegans*. Cell *119*, 209–218.

Hogan, B., Costantini, F., Beddington, R., and Lacy, E. (1994). Manipulating the Mouse Embryo: A Laboratory Manual, Second edition (Plainview, NY: Cold Spring Harbor Laboratory Press).

Huang, L., Mivechi, N.F., and Moskophidis, D. (2001). Insights into regulation and function of the major stress-induced hsp70 molecular chaperone in vivo: analysis of mice with targeted gene disruption of the hsp70.1 or hsp70.3 gene. Mol. Cell. Biol. *21*, 8575–8591.

Hunt, P., LeMaire, R., Embury, P., Sheean, L., and Mroz, K. (1995). Analysis of chromosome behavior in intact mammalian oocytes: monitoring the segregation of a univalent chromosome during female meiosis. Hum. Mol. Genet. *4*, 2007–2012.

Kimple, R.J., Kimple, M.E., Betts, L., Sondek, J., and Siderovski, D.P. (2002). Structural determinants for GoLoco-induced inhibition of nucleotide release by Galpha subunits. Nature *416*, 878–881.

Lee, J.H., Yoon, S.Y., and Bae, I.H. (2004). Studies on Ca(2+)-channel distribution in maturation arrested mouse oocyte. Mol. Reprod. Dev. *69*, 174–185.

Miller, K.G., and Rand, J.B. (2000). A role for RIC-8 (Synembryn) and GOA-1 (G(o)alpha) in regulating a subset of centrosome movements during early embryogenesis in *Caenorhabditis elegans*. Genetics *156*, 1649–1660.

Neubig, R.R., and Siderovski, D.P. (2002). Regulators of G-protein signalling as new central nervous system drug targets. Nat. Rev. Drug Discov. *1*, 187–197.

Schaefer, M., Petronczki, M., Dorner, D., Forte, M., and Knoblich, J.A. (2001). Heterotrimeric G proteins direct two modes of asymmetric cell division in the *Drosophila* nervous system. Cell *107*, 183–194.

Schultz, R.M. (2002). The molecular foundations of the maternal to zygotic transition in the preimplantation embryo. Hum. Reprod. Update *8*, 323–331.

Schweitzer, J.K., and D'Souza-Schorey, C. (2002). Localization and activation of the ARF6 GTPase during cleavage furrow ingression and cytokinesis. J. Biol. Chem. *277*, 27210–27216.

Snow, B.E., Antonio, L., Suggs, S., Gutstein, H.B., and Siderovski, D.P. (1997). Molecular cloning and expression analysis of rat Rgs12 and Rgs14. Biochem. Biophys. Res. Commun. *233*, 770–777.

Srinivasan, D.G., Fisk, R.M., Xu, H., and van den Heuvel, S. (2003). A complex of LIN-5 and GPR proteins regulates G protein signaling and spindle function in *C. elegans*. Genes Dev. *17*, 1225–1239.

Tall, G.G., Krumins, A.M., and Gilman, A.G. (2003). Mammalian Ric-8A (synembryn) is a heterotrimeric Galpha protein guanine nucleotide exchange factor. J. Biol. Chem. *278*, 8356–8362.

Traver, S., Bidot, C., Spassky, N., Baltauss, T., De Tand, M.F., Thomas, J.L., Zalc, B., Janoueix-Lerosey, I., and Gunzburg, J.D. (2000). RGS14 is a novel Rap effector that preferentially regulates the GTPase activity of galphao. Biochem. J. *350*, 19–29.

Willard, F.S., Kimple, R.J., and Siderovski, D.P. (2004). Return of the GDI: the GoLoco motif in cell division. Annu. Rev. Biochem. *73*, 925–951.